Alcohol dehydrogenase 4 is a TP53-associated gene signature for the prediction of prognosis in hepatocellular carcinoma

YUAN ZHANG[1,2], HUI-HONG JIANG[1], ZHEN-YU WANG[3], BO ZHAI[3*] and MOU-BIN LIN[1*]

[1]Department of General Surgery, Yangpu Hospital, School of Medicine, Tongji University, Shanghai 200090; [2]Department of Gynecology and Obstetrics, International Peace Maternity and Child Health Hospital, School of Medicine, Shanghai Jiao Tong University, Shanghai 200030; [3]Department of Interventional Oncology, Renji Hospital, School of Medicine, Shanghai Jiao Tong University, Shanghai 200127, P.R. China

Received June 14, 2022; Accepted October 12, 2022

DOI: 10.3892/ol.2022.13589

Abstract. Tumor protein p53 (TP53) is one of the most frequently mutated genes in hepatocellular carcinoma (HCC), an event that has been associated with a poor prognosis. Therefore, availability of an accurate prognostic signature would be beneficial for improving therapeutic efficacy and patient prognosis. In the present study, HCC genetic mutation data, transcriptomic data and clinical data were downloaded from The Cancer Genome Atlas database to screen for specific TP53-associated signatures based on differentially expressed genes. Subsequently, the predictive value of any signatures found for the overall survival (OS) and the immune response were investigated, followed by validation in clinical specimens. The present study revealed 270 mutant genes, of which 28% were TP53 mutations. In addition, 81 upregulated genes and 27 downregulated genes were identified. Enrichment analysis revealed that mutant TP53 was particularly enriched for pathways associated with the cell cycle and cell metabolism, and whilst clustered, most enriched for terms associated with metabolic processes and the immune response. The alcohol dehydrogenase 4 (ADH4) gene was selected using univariate and multivariate Cox regression analysis. A nomogram was constructed to validate this prognostic signature. Patients in the low-ADH4 expression group displayed significantly worse OS time regardless of the TP53 mutation status compared with the high-ADH4 expression group. In addition, a higher degree of B-cell infiltration was observed in the low-ADH4 expression group, revealing differential immune microenvironments. Subsequently, ADH4 expression and the prognostic prediction values were validated further in clinical HCC samples by IHC assay, Risk score, OS analysis and ROC analysis. To conclude, these data suggest that the TP53-associated immune-metabolic signature is a specific and independent prognostic biomarker for patients with HCC that will help to facilitate novel immunotherapy development.

Correspondence to: Dr Mou-Bin Lin, Department of General Surgery, Yangpu Hospital, School of Medicine, Tongji University, 450 Tengyue Road, Shanghai 200090, P.R. China
E-mail: 1500142@tongji.edu.cn

Dr Bo Zhai, Department of Interventional Oncology, Renji Hospital, School of Medicine, Shanghai Jiao Tong University, 160 Pujian Road, Shanghai 200127, P.R. China
E-mail: zhaiboshi@sina.com

*Contributed equally

Abbreviations: ADH4, alcohol dehydrogenase 4; DEG, differentially expressed gene; GO, Gene Ontology; HCC, hepatocellular carcinoma; ICB, immune checkpoint blockage; OS, overall survival; TCGA, The Cancer Genome Atlas; TME, tumor microenvironment; TP53, tumor protein p53

Key words: ADH4, HCC, immunometabolism, prognosis, TP53

Introduction

Hepatocellular carcinoma (HCC) is one of the most aggressive malignancies among all types of cancer and constitutes >75% of liver cancer cases, which in turn accounts for 4.7% of the total cancer cases in the world (1). Asia has the highest incidence of liver cancer, with China accounting for 47% of the world's burden (2). Over previous decades, the incidence of HCC has increased whilst the prognosis has remained poor, as a result of high rates of recurrence and metastasis (3,4). At present, clinical outcomes of patients with HCC remain unsatisfactory, although progress has been made towards the prevention of this disease. For example, the 5-year survival of HCC was only 18% in the USA in 2014 (5). Accumulating evidence indicates that the phenotype of each individual tumor is regulated by its tumor microenvironment (TME) (6-8). As an immune-sensitive organ, the liver exerts powerful metabolic functions. A number of studies have previously found that the immune system can exert regulatory metabolic functions in a manner that was not previously recognized, giving rise to a novel research field called immunometabolism (9-11). However, at present, studies that have systematically explored this relationship between the immunometabolism of the TME and its prognosis remain scarce.

As a transcription factor, tumor protein p53 (TP53) inhibits cell division and survival, thereby functioning as a key fail-safe mechanism in the cellular anticancer defense

system (12). Therefore, the TP53 gene has been frequently found to be mutated in human malignancies, which leads to its proposal for use as a potential predictive marker and/or target for therapeutic intervention (13-15). Previous studies have revealed that TP53 mutations in various cancer types, such as breast and ovarian, are associated with increased resistance to cancer therapies and poor prognoses (16,17). Therefore, unraveling the association between alterations in the TME immunometabolism following TP53 mutation and prognosis would be of significance, especially for HCC.

In the present study, it was hypothesized that the overall survival (OS) time of patients with HCC harboring TP53 mutations may be influenced by immunometabolism in the TME. Therefore, genes that are affected by TP53 mutations were investigated, and these were used to establish an immune-metabolism gene signature to predict the prognosis of patients with HCC in the clinic.

Materials and methods

Collection of genome-wide mutation data. In the present study, HCC genetic mutation profile, transcriptomic and clinical data were all downloaded by searching the Project ID 'TCGA-LIHC' using The Cancer Genome Atlas (TCGA; https://portal.gdc.cancer.gov/). In the section of Cases and File Counts by Experimental Strategy, 371 cases containing both clinical information and RNA sequence data were selected and saved. Mutation data were visualized using the 'maftools' package (v2.12.0, bioconductor.org/packages/release/bioc/html/maftools.html) in R software (v4.0.3, https://mran.microsoft.com/snapshot/2020-12-04/bin/windows/base/). MutsigCV represents mutation significance covariants.

Screening and gene enrichment analysis of differentially expressed genes (DEGs). The 'Limma' package (v3.52.4, bioconductor.org/packages/release/bioc/html/limma.html) of R software was used to screen for DEGs, whereas the 'ClusterProfiler' package (v3.0.4, https://rdocumentation.org/packages/clusterProfiler/versions/3.0.4) was used to analyze the Kyoto Encyclopedia of Genes and Genomes pathways and the Gene Ontology (GO) functions. $P<0.05$ and $-1>\log(\text{fold-change})>1$ were considered to be the thresholds.

Selection of a specific signature. Univariate and multivariate Cox regression analyses were performed and the 'forestplot' package (v1.10.1, https://rdocumentation.org/packages/forestplot/versions/1.10.1) was used to show the P-values, hazard ratios and 95% confidence intervals of each variable. $P<0.05$ was considered to be the threshold. A nomogram based on the results of the multivariate Cox analysis, and a list of proposed risk factors found using the 'rms' package (v6.1-0, https://rdocumentation.org/packages/rms/versions/6.1-0), was then constructed to predict the 1-, 3- and 5-year OS rates. If Kaplan-Meier curves crossed over, a two-stage procedure was performed using the 'TSHRC' package (v0.1-6, https://cran.r-project.org/web/packages/TSHRC/index.html) of R software. Analyses of risk score, survival status and heatmaps were implemented using the 'ggrisk' package (v1.3, https://cran.r-project.org/web/packages/ggrisk/) of R software. The time receiver operating characteristic analysis was used to compare the predictive accuracy of alcohol dehydrogenase 4 (ADH4). All analytical methods were performed using R software (version 4.0.3) with the 'ggplot2' package (v3.3.3, https://rdocumentation.org/packages/ggplot2/versions/3.3.3). $P<0.05$ was considered to indicate a statistically significant difference.

Estimation of immune cell score and immune infiltration. The 'immunedeconv' package (v2.0.3; rdocumentation.org/packages/immunedeconv/versions/2.0.3) of R software was used to integrate the Estimating the Proportions of Immune and Cancer cells algorithm to estimate the immune cell score and immune infiltration. CD274, cytotoxic T-lymphocyte-associated protein 4 (CTLA4), hepatitis A virus cellular receptor 2 (HAVCR2), lymphocyte activating 3 (LAG3), programmed cell death protein 1 (PDCD1), programmed cell death protein 1 ligand 2 (PDCD1LG2), T cell immunoreceptor with Ig and immunoreceptor tyrosine-based inhibitory motif domains, and sialic acid binding Ig-like lectin 15 were selected to be the immune checkpoint-associated relevant transcripts, before their expression values were extracted. Analyses were implemented using R software (version 4.0.3) with 'ggplot2' and 'pheatmap' packages (v1.0.12, https://rdocumentation.org/packages/pheatmap/versions/1.0.12).

Collection of HCC specimens. Surgically resected specimens were obtained in October 2021 from 3 patients with HCC at Renji Hospital Affiliated with Shanghai Jiao Tong University School of Medicine (Shanghai, China). The inclusion criteria included: i) Pathological diagnosis of HCC; ii) the patient had received no prior treatment; and iii) the patient accepted surgical resection without distant disease. The exclusion criteria included: i) Other types of primary liver cancer; and ii) the patient refused the surgical resection. Tissue within 2 cm from the tumor boundary is called adjacent tissue. All specimens were conserved in liquid nitrogen. The present study was approved by the Ethics Committee of Renji Hospital (Shanghai, China) and written informed consent was provided by the enrolled patients.

Immunohistochemistry. ADH4 protein expression was examined using an immunohistochemistry assay. Fresh specimens were fixed in 4% phosphate-buffered formalin for at least 24 h at room temperature. All HCC tissues were paraffin-embedded and cut into 4-μm-thick sections. The sections were then dewaxed with xylene and rehydrated with descending graded alcohol. Activity of endogenous catalase would be inhibited by 0.3% H_2O_2. Heat-mediated antigen retrieval of tissue sections was performed at 98˚C and maintained for 20 min before the sections were allowed to cool. After blocking non-specific sites with 5% goat serum at 37˚C for 30 min, the sections were incubated with anti-ADH4 primary antibody (cat. no. Ab137077; 1:500 dilution; Abcam) overnight at 4˚C and then with HRP-conjugated goat anti-rabbit secondary antibody (cat. no. Ab6721; 1:1,000 dilution; Abcam) for 1 h at room temperature. Antibodies were visualized using 3,3'-diaminobenzidine and counterstained using Meyer's Hematoxylin for 2 min at room temperature. Sections were then dehydrated using an increasing gradient of alcohols before being cleared in xylene.

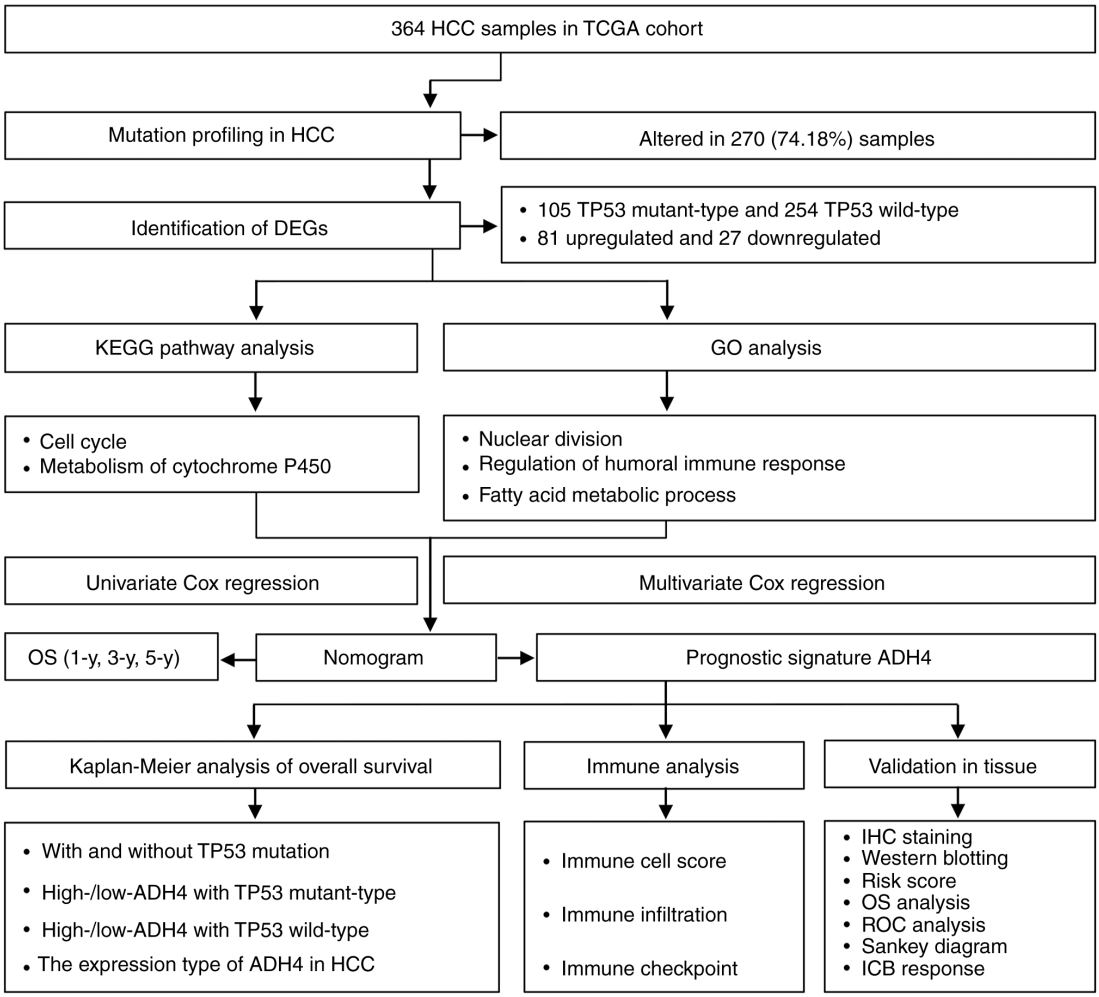

Figure 1. Flowchart of the present study. ADH4, alcohol dehydrogenase 4; DEG, differentially expressed gene; GO, Gene Ontology; HCC, hepatocellular carcinoma; ICB, immune checkpoint blockage; IHC, immunohistochemistry; KEGG, Kyoto Encyclopedia of Genes and Genomes; OS, overall survival; ROC, receiver operating characteristic; TCGA, The Cancer Genome Atlas; TP53, tumor protein p53; y, years (371 cases were saved and only 364 samples were listed, because 8 cases was deleted due to incomplete information).

Images were observed using a light Olympus Corporation BX51 instrument. The difference of immunostaining results were evaluated using Image J software (v1.52a, USA).

Western blotting. ADH4 protein expression of the resected tissues was examined using western blotting. The tissues were first treated using a lysis solution (RIPA, Radio-Immunoprecipitation Assay buffer; Thermo Fisher Scientific, USA), which contained 1% (v/v) protease inhibitors (cat. no. P8340; Merck KGaA) to extract protein samples. The protein concentration was measured and normalized using Protein Quantification kit (BCA Assay; Beyotime, China). Western blot analysis was then performed as previously described (18). The membranes were blocked in Tris-Buffer Saline Tween 20 (1xTBST) containing 5% non-fat milk at room temperature for 45 min. Then, membranes would be incubated with anti-ADH4 primary antibody (cat. no. Ab137077; 1:1,000 dilution; Abcam) overnight at 4˚C and HRP-conjugated goat anti-rabbit secondary antibody (cat. no. Ab6721; 1:1,000 dilution; Abcam) for 1 h at room temperature. Enhanced chemiluminescence reagent (SuperSignal™ West Atto Ultimate Sensitivity Substrate; Thermo Fisher Scientific, Inc.) was used for immunodetection. The level of actin protein expression was measured as an internal standard (anti-β actin antibody; cat. no. Ab8227; 1:1,000 dilution; Abcam). The density of protein band was quantitatively measured using Image J software (v1.52a, USA).

Immune checkpoint blockage (ICB) response prediction. Potential ICB responses were predicted using the Tumor Immune Dysfunction and Exclusion algorithm (19) and software packages 'ggplot2' and 'ggpubr' (v0.4.0, https://rdocumentation.org/packages/ggpubr/versions/0.4.0). All analytical methods were performed using R software (version 4.0.3). $P<0.05$ was considered to indicate a statistically significant difference.

Statistical analysis. All statistical analyses were performed using R software (version 4.0.3). Unpaired Student's t-test was used to compare any differences between the subgroups in DEGs analysis. Data from two groups were compared in cox regression and K-M curve analysis using the Wilcoxon rank-sum test, whereas more than three groups were compared in immune analysis using the Kruskal-Wallis

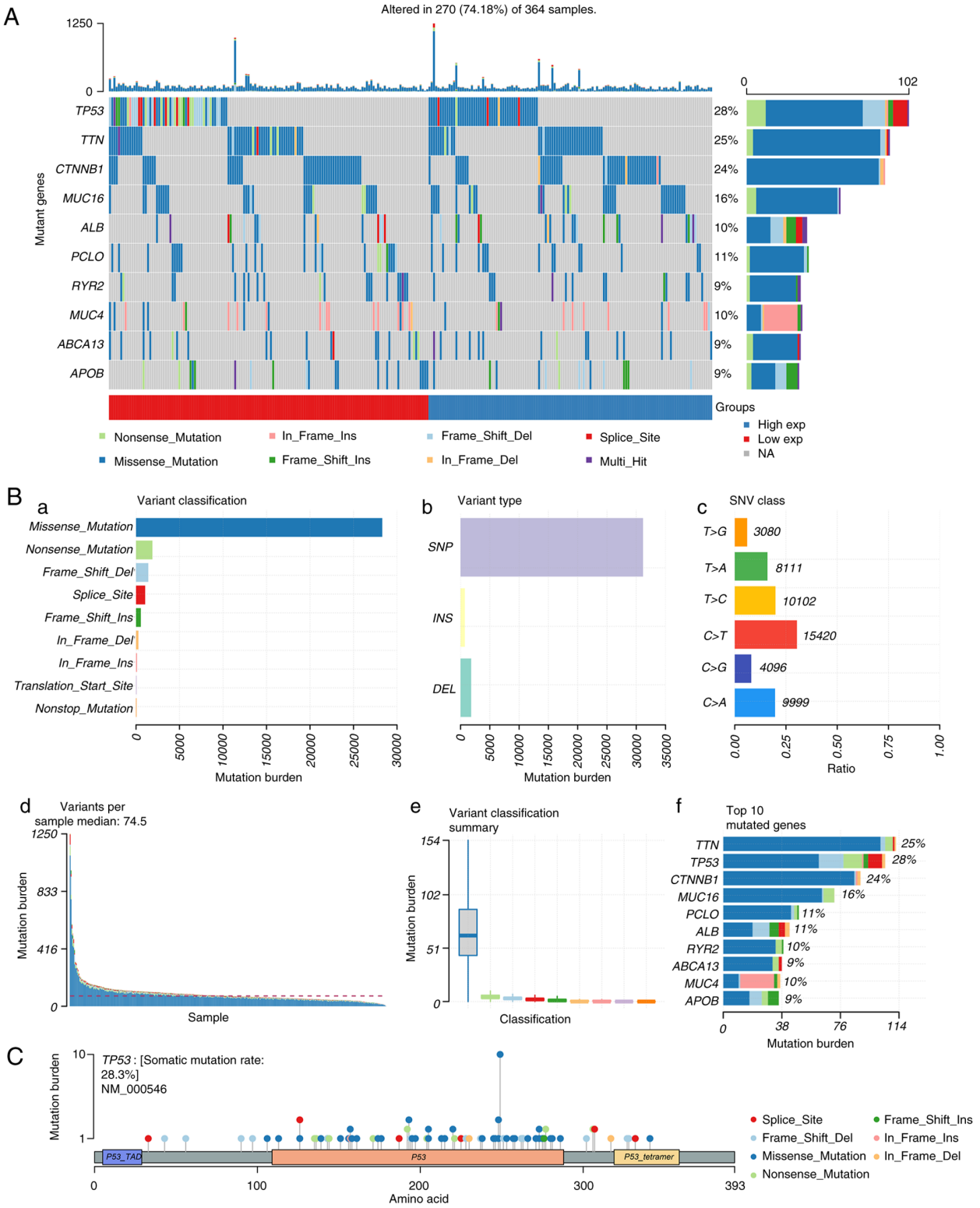

Figure 2. Genome-wide mutation profiling in HCC. (A) Oncoplot (left) displaying the somatic landscape of the HCC cohort. Genes are ordered by their mutation frequency and samples are ordered according to disease histology as indicated by the annotation bar (bottom). The bar plot (right) shows log10 transformed Q-values estimated by MutSigCV. (B) Cohort summary plot displaying the distribution of variants according to (a) variant classification, (b) variant type and (c) SNV class. (d) Mutation load of each sample and (e) variant classification type. (f) Top 10 mutant genes. (C) Lollipop plot displaying mutation distribution and protein domains for TP53 in HCC, with labeled recurrent hotspots. Somatic mutation rate and transcript names are indicated by the plot title and subtitle, respectively. Del, deletion; exp, expression; HHC, hepatocellular carcinoma; Ins, insertion; NA, not available; SNP, single nucleotide polymorphism; SNV, single nucleotide variant; TAD, transaction domain; TP53, tumor protein p53.

test. Post hoc test was performed using Least Significance Difference method. Data are presented by mean and SD. χ-square test was used to compare significant differences between groups. P<0.05 was considered to indicate a statistically significant difference. Test was performed no less than three independent repeats.

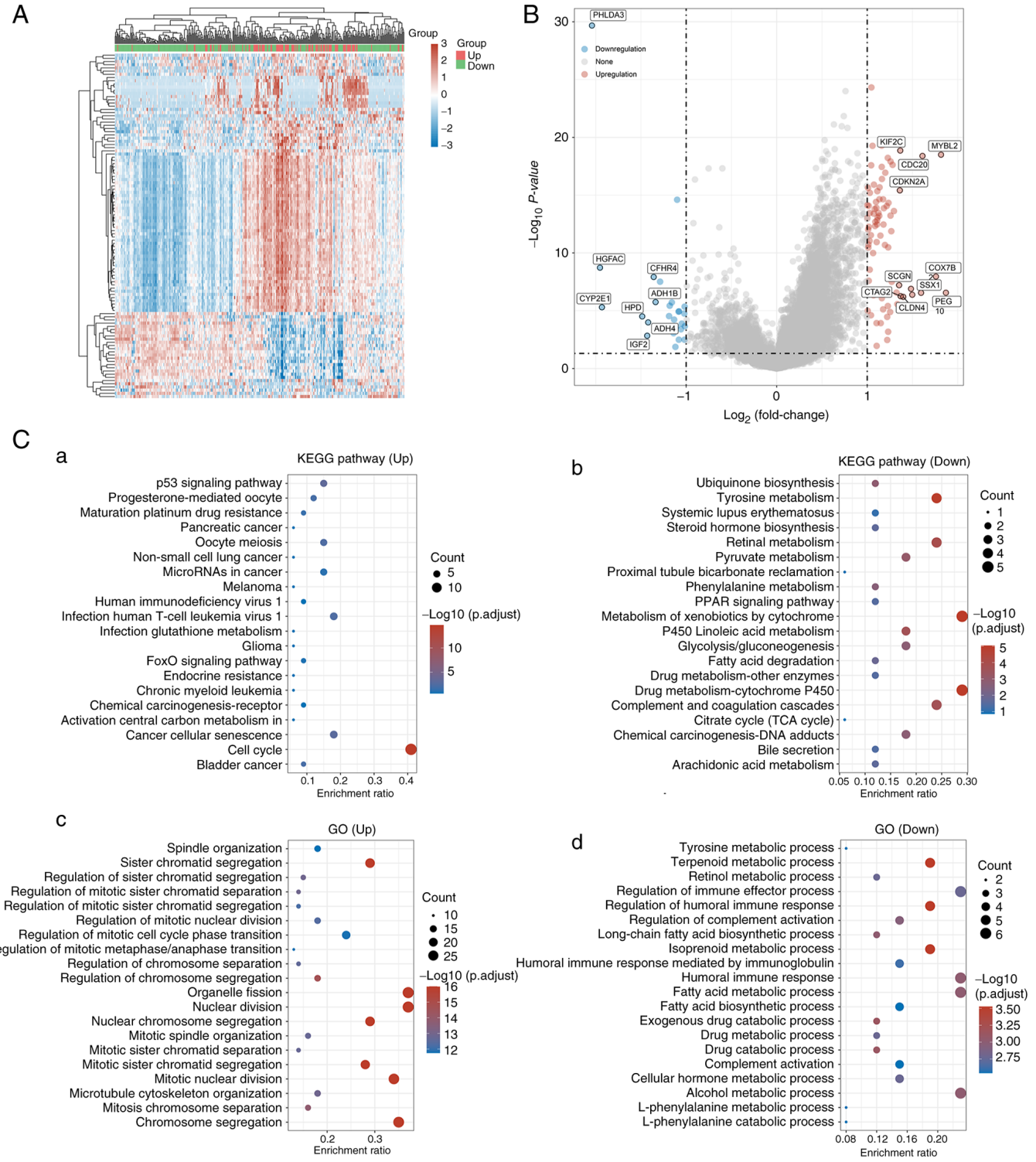

Figure 3. Identification of DEGs in patients with and without tumor protein p53 mutations in hepatocellular carcinoma. (A) Heatmap of DEGs. (B) Volcano plots of DEGs. (C) Enriched KEGG signaling pathways of primary biological actions of target (a) upregulated and (b) downregulated mRNAs and GO analysis of potential targets of (c) upregulated and (d) downregulated mRNAs. P<0.05 was considered to be enriched to a significantly different pathway. DEG, differentially expressed gene; GO, Gene Ontology; KEGG, Kyoto Encyclopedia of Genes and Genomes.

Results

TP53 is the most frequently mutated gene in HCC. The experimental plan of the present study is presented in Fig. 1. A total of 270 mutant genes in HCC were screened from TCGA. Mutant genes revealed by the screen, including TP53 (28%), Titin (25%), Catenin Beta 1 (24%), mucin 16 (16%) and piccolo presynaptic cytomatrix protein (11%), had higher mutation frequencies than the rest of screened mutant genes, which is demonstrated by the horizontal histogram (Fig. 2A). In particular, missense mutations appeared to be the most common type of TP53 mutation (Fig. 2Ba). Single-nucleotide polymorphisms showed a predominant position compared with deletions or insertions (Fig. 2Bb). C>T was found to

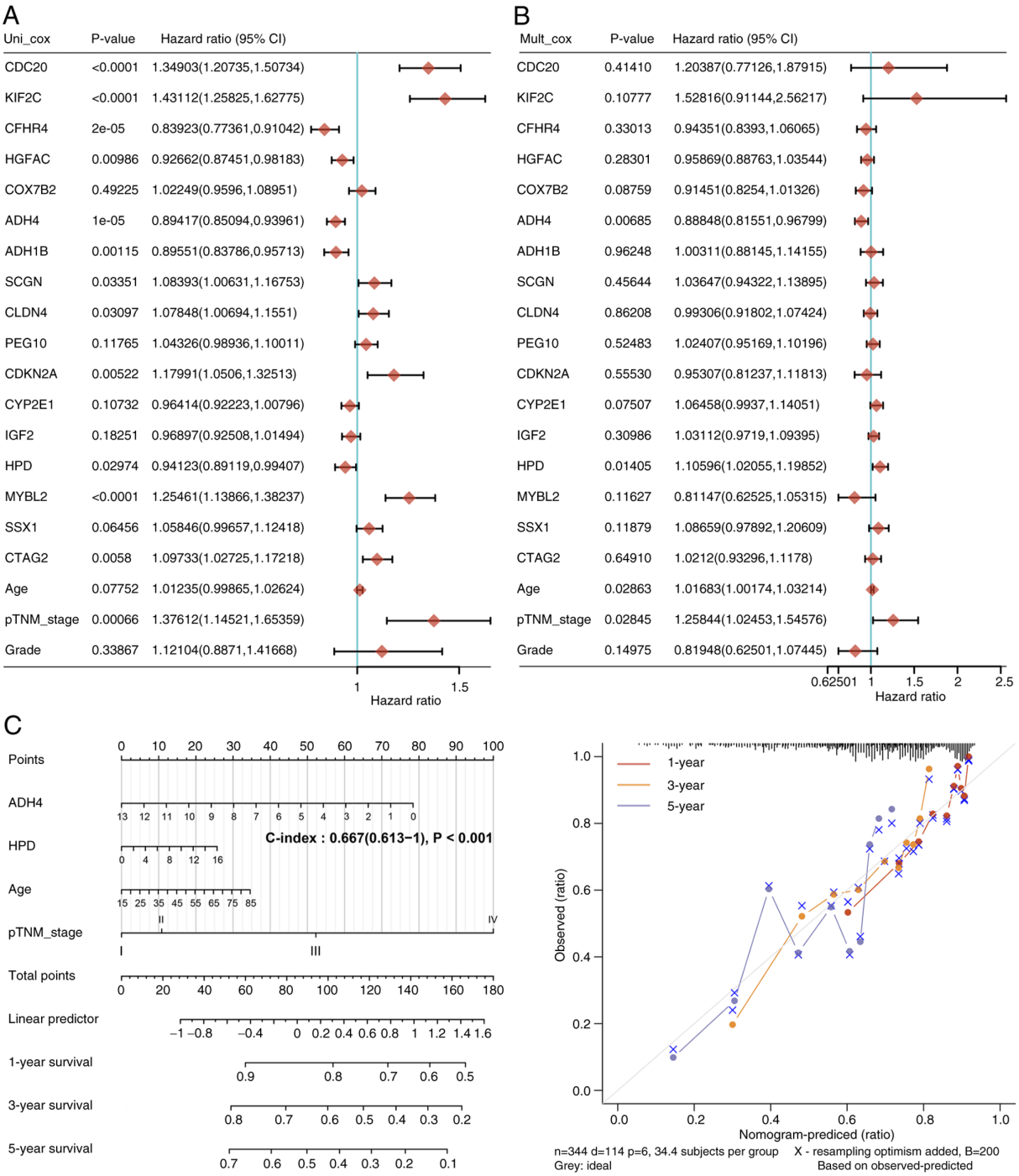

Figure 4. Construction of a prognostic signature based on DEGs. Prognostic values of DEGs in (A) univariate and (B) multivariate cox regression analysis. (C) Nomogram to predict the 1-, 3- and 5-year OS of patients with hepatocellular carcinoma. The grey line represents the ideal nomogram, and the red, orange and blue lines represent the 1-, 3- and 5-year observed nomograms, respectively. ADH4, alcohol dehydrogenase 4; DEGs, differentially expressed genes; OS, overall survival.

be the most distinct mutation type (Fig. 2Bc). The number of mutations per sample is shown in Fig. 2Bd. Each color in the box diagram represents one type of mutation (Fig. 2Be). Fig. 2Bf shows the top 10 mutant genes and TP53 is ranked second. Fig. 2C presents a lollipop plot, which shows that TP53 a highly mutated gene in HCC and missense mutations is the most common type of TP53 mutation.

DEGs detected in HCC by TP53 status. DEGs between the TP53 mutant and wild-type TP53 groups were next screened. In total, 81 upregulated genes and 27 downregulated genes were identified (Fig. 3A and B). Notably, 'tyrosine metabolism' and 'pyruvate metabolism' were markedly downregulated, in addition to 'alcohol metabolic process' and 'regulation of immune effector process' (Fig. 3C). By contrast, mutant TP53 was particularly enriched for pathways associated with the 'cell cycle' and cell metabolism, 'cytochrome metabolism and drug metabolism (Fig. 3Ca and Cb). Furthermore, genes associated with TP53 mutation tended to be more enriched for terms associated with the metabolic process, including nuclear

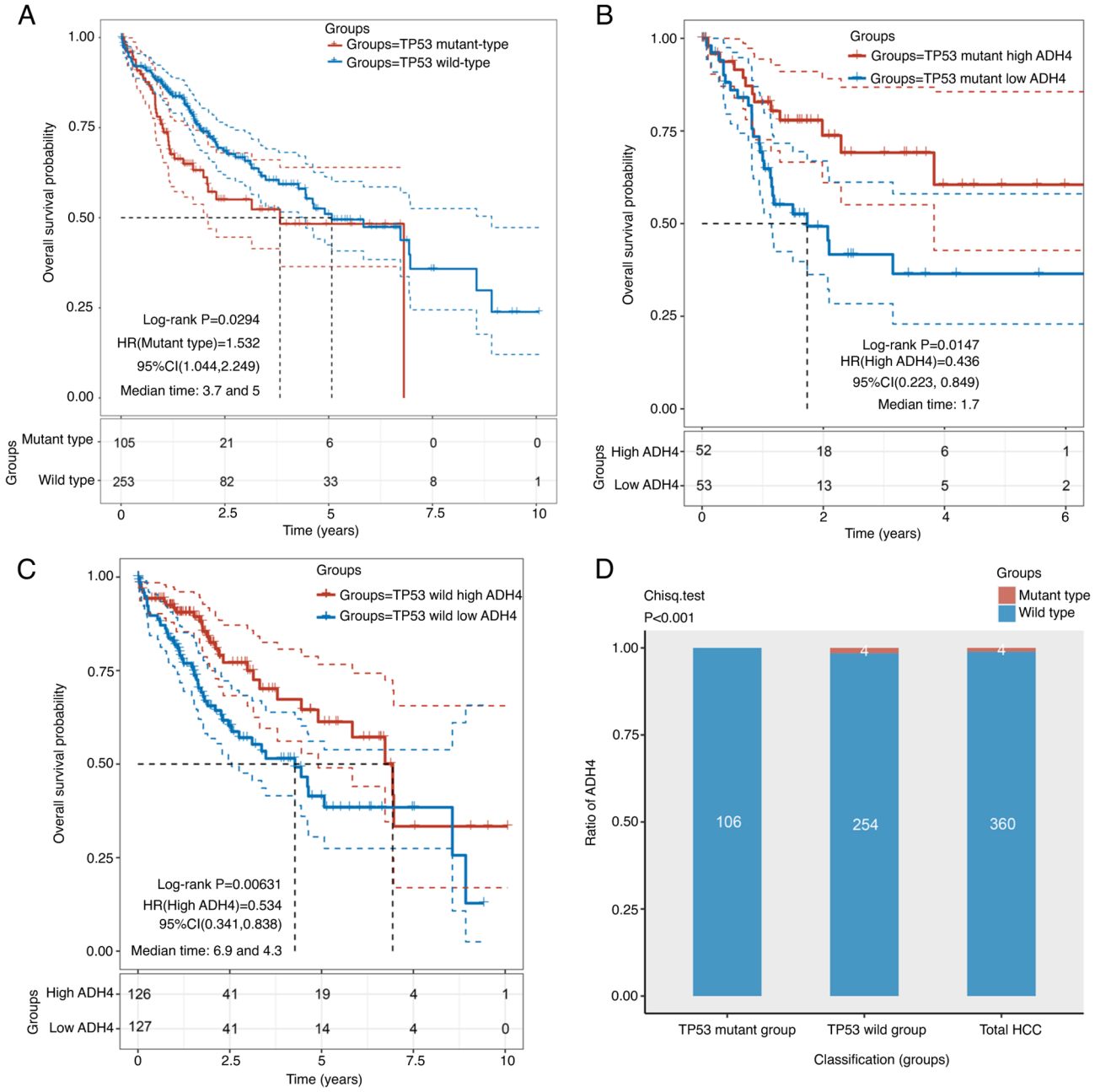

Figure 5. Kaplan-Meier analysis of overall survival according to TP53 mutation and ADH4 status. (A) Kaplan-Meier survival by TP53 status. (B) Kaplan-Meier survival in the TP53 mutant group by ADH4 status. (C) Kaplan-Meier survival in the TP53 wild-type group by ADH4 status. (D) NExpression type of ADH4 mRNA in different groups of HCC (chi-q. test). ADH4, alcohol dehydrogenase 4; HCC, hepatocellular carcinoma; HR, hazard ratio; TP53, tumor protein p53. Dotted lines represent the confidence interval.

division and humoral immune response (Fig. 3Cc and Cd). These results suggested that genes associated with TP53 mutations are likely to serve an important role in the immuno-metabolism of the TME in HCC.

ADH4 is a prognostic signature for HCC. A total of 17 genes and corresponding clinical information, including age, pTNM_stage and grade were identified through univariate (Fig. 4A) and multivariate (Fig. 4B) Cox regression analyses, to build a predictive nomogram. The predictors included ADH4, 4-hydroxyphenylpyruvate dioxygenase, patient age and pathological Tumor-Node-Metastasis (pTNM) stage (20) (Fig. 4C), all of which met the P<0.05 criteria during risk assessment. The P-value of ADH4 was found to be <0.001, which suggested that ADH4 can be exploited as a distinct prognostic signature for HCC. The calibration plots for the 1-, 3- and 5-year OS rates were consistent compared with those predicted by the ideal model in the entire cohort (Fig. 4C).

TP53 and ADH4 status are associated with the prognosis of HCC. The mutant TP53 and wild-type TP53 groups included 105 and 253 patients, respectively. Patients in the mutant TP53 group displayed significantly worse OS time compared with those in the wild-type group (Fig. 5A). To investigate if ADH4 was independent of the TP53 mutation status, patients with HCC were divided into high- and low-ADH4 groups based on

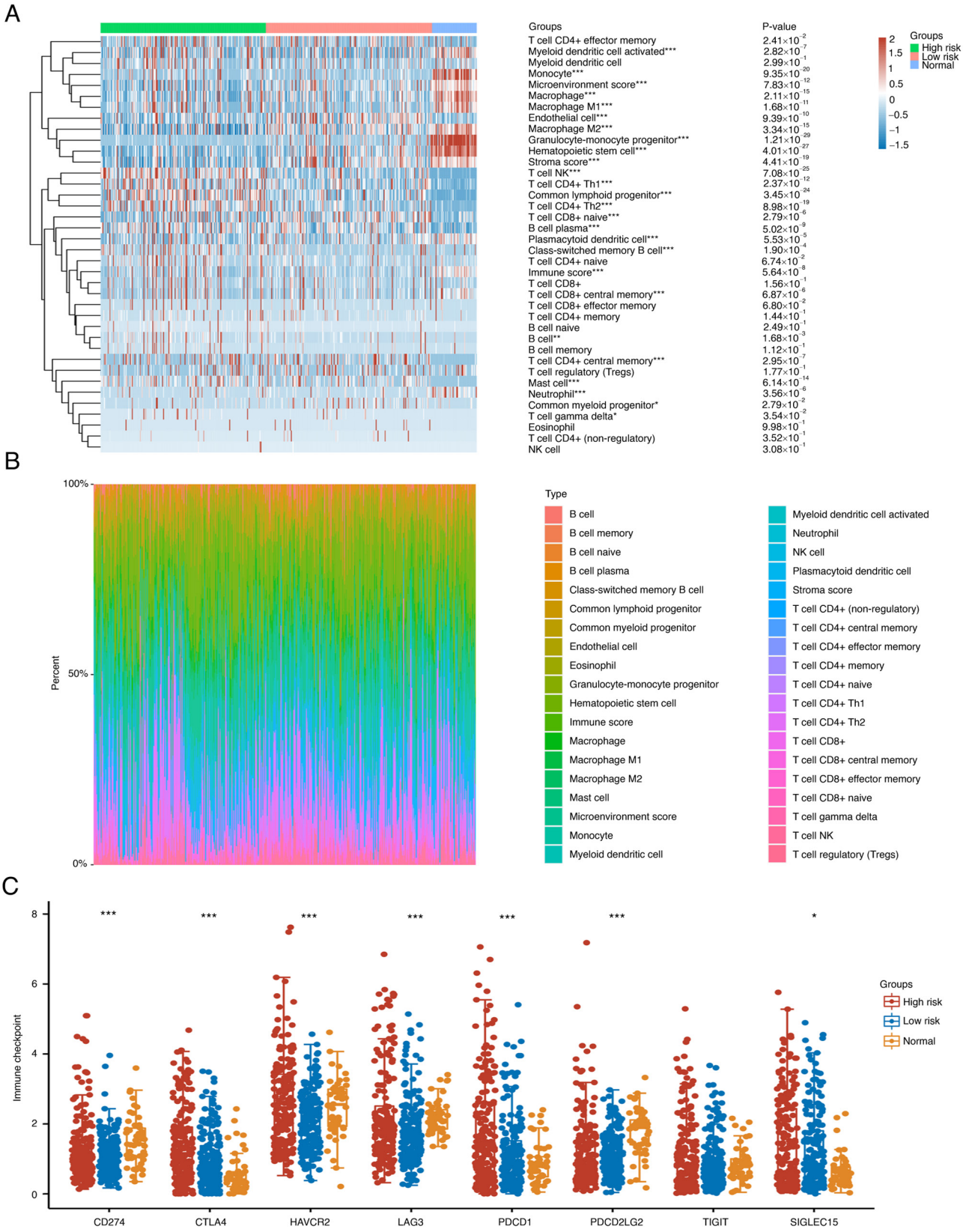

Figure 6. Immune analysis of high- and low-risk patients with hepatocellular carcinoma (A) Heat map of immune cell score. (B) Percentage abundance of tumor-infiltrating immune cells. The abscissa represents the sample and the ordinate represents the percentage of immune cell content in a single sample. (C) Expression distribution of immune checkpoint markers in tissues. *P<0.05, **P<0.01 and ***P<0.001.

the TP53 mutation status. The high- and low-ADH4 groups in the mutant TP53 group included 52 and 53 patients, respectively. By contrast, the high- and low-ADH4 groups in the wild-type TP53 group included 126 and 127 patients, respectively. The results revealed that the low-ADH4 group in both the mutant and wild-type TP53 groups displayed significantly worse OS

Table I. Clinicopathological information of 3 patients with HCC.

Case	Age, years	Sex	Ethnicity	Tumor type	Pathological type	Edmondson-Steiner grade (39)	TP53 status	Vital status
1	48	Male	Asian	Primary tumor	HCC	III	Mutation (serine 249)	Alive
2	62	Male	Asian	Primary tumor	HCC	III	Mutation (serine 249)	Alive
3	55	Male	Asian	Primary tumor	HCC	IV	Mutation (serine 249)	Alive

HCC, hepatocellular carcinoma; TP53, tumor protein p53.

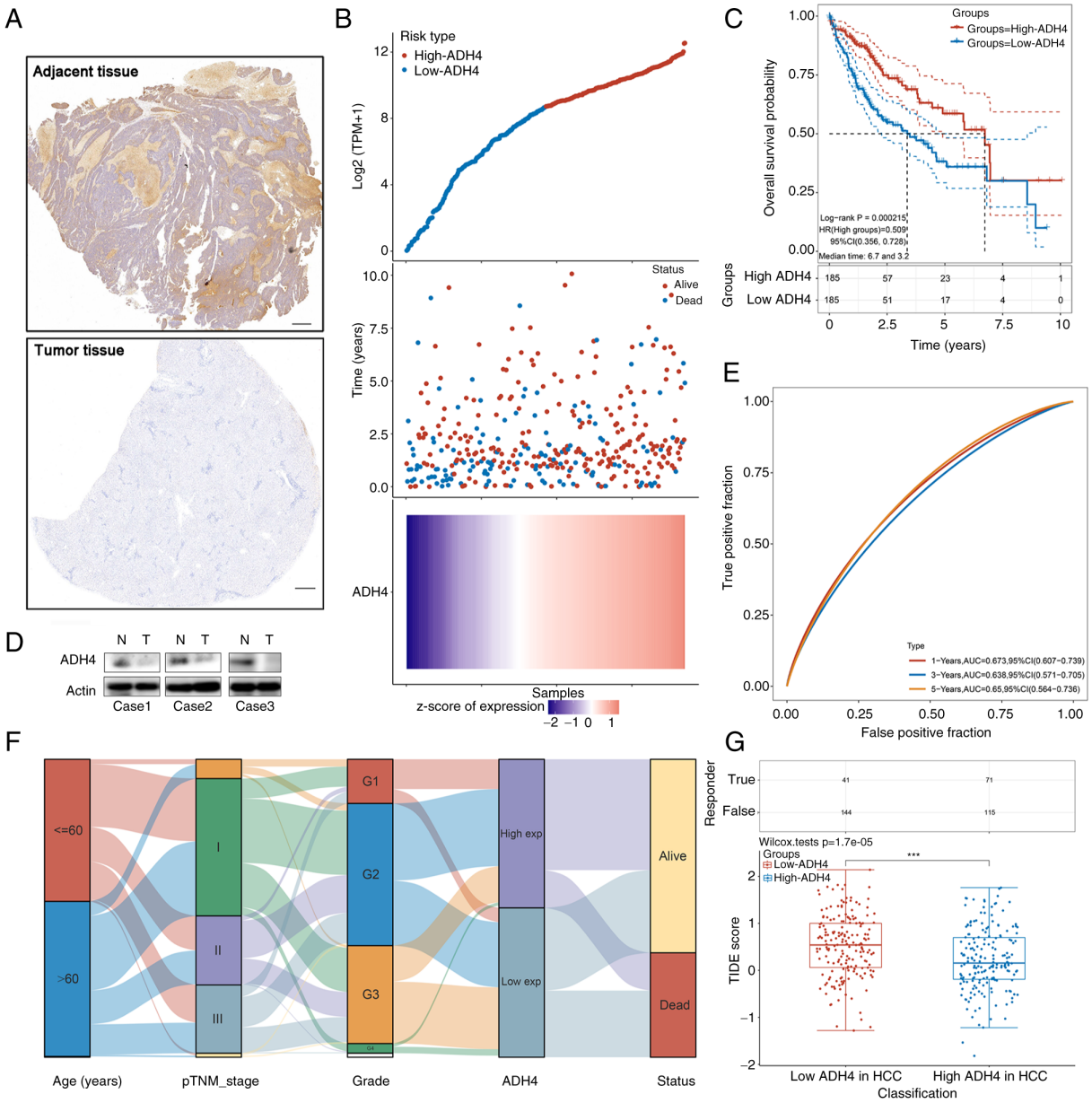

Figure 7. Validation of gene signature in clinical HCC tissue samples. (A) Representative images of immunohistochemistry staining for ADH4 expression in adjacent non-tumor tissues (top) and HCC tissues (bottom). Scale bar, 500 μm. (B) Curve of risk score (top), the survival status of the patients (middle) and the heatmap of the ADH4 expression profile (bottom). (C) Kaplan-Meier survival analysis of patients with HCC by ADH4 status. Dotted lines represent the confidence interval. (D) Western blot analysis of adjacent non-tumor and HCC tissues. (E) Time-dependent receiver operating characteristic analysis of the ADH4 signature. (F) Sankey diagram of ADH4 expression, which indicates the distribution of the same sample in different characteristic variables including ages, pTNM_stages, grade, ADH4 expression type and status of patients. (G) Potential immune checkpoint blockage responses of HCC groups by their ADH4 status, which indicates the distribution of immune response scores in different groups in the prediction results (***P<0.001). The upper table indicates the positive immune response amount in the samples. ADH4, alcohol dehydrogenase 4; AUC, area under the curve; exp, expression; HCC, hepatocellular carcinoma; HR, hazard ratio; N, normal; T, tumor; pTNM, pathological Tumor-Node-Metastasis; TPM, transcript per million; TIDE, Tumor Immune Dysfunction and Exclusion.

time compared with the high-ADH4 group (Fig. 5B and C). The crossed curves in Fig. 5 were determined to be statistically different (Fig. 5A, P=0.0294; Fig. 5B, P=0.0147; Fig. 5C, P=0.0063;) by performing a two-stage procedure, using the 'TSHRC' package of R software. In addition, wild-type ADH4 was observed to occupy a particularly higher proportion of patients with HCC than mutant type ADH4 (χ^2 test; Fig. 5D).

Differential immune analysis. According to the results in Fig. 5, high risk group in Fig. 6 was defined as low ADH4 expression while low risk group in Fig. 6 was defined as high ADH4 expression. To explore the distribution of immune scores (Fig. 6A) and immune infiltration (Fig. 6B) in the groups of different risks, 38 types of immune cells were compared in total. Among them, 23 types of immune cells were found to be statistically different from other rest 15 types of immune cells. It was noted that there was significant immune infiltration by cells expressing markers of B cells in the high-ADH4 group than other immune cells in the Fig. 6B, whilst the expression of markers of T cells was decreased, suggesting a differential immune TME. For the expression distribution of immune checkpoint markers in the HCC tissues, CD274, CTLA4, HAVCR2, LAG3, PDCD1, PDCD1LG2, TIGIT and SIGLEC15 were discovered to be the immune checkpoint-associated transcripts showing a statistical difference, which was different from other transcripts (Fig. 6C).

ADH4 expression was validated in clinical HCC tissues. To validate the identified gene signature, ADH4 expression levels were examined using immunohistochemistry and western blotting on pairs of HCC tissues and adjacent normal tissues from 3 patients. The pathological diagnosis of the 3 male patients was HCC without distant metastasis, and none had received any prior treatment. The clinicopathological information of the 3 patients is shown in Table I. The TP53 status of these patients was mutant type and the molecular hallmark was a mutation at codon 249 in TP53. The results demonstrated that ADH4 protein expression was markedly increased in the normal tissues compared with the tumor tissues (Fig. 7A and D). The risk score of every patient whose RNA Seq files was downloaded from TCGA was then calculated to obtain the median cut-off point to divide them into the high-ADH4 group (n=185) and low-ADH4 group (n=185) (Fig. 7B, top). The survival status of all patients with HCC is shown (Fig. 7B, middle) and the prognostic ADH4 gene expression profile is shown in the heatmap (Fig. 7B, bottom). The Kaplan-Meier survival curves demonstrated that patients in the low-ADH4 group had worse OS time compared with those in the high-ADH4 group (Fig. 7C, P=0.0002). In addition, a time-dependent receiver operating characteristic analysis suggested that ADH4 expression had accurate predictive capabilities for 1-, 3- and 5-year OS (Fig. 7E). A Sankey diagram of ADH4 expression revealed the distribution of the same sample in different characteristic variables including ages, pTNM_stages, grade, ADH4 expression type and status of patients (Fig. 7F). Potential ICB responses indicated that the distribution of the TIDE scores in the low-ADH4 group showed a worse response compared with that in the high-ADH4 group (Fig. 7G).

Discussion

HCC is one of the main causes of cancer-associated mortality worldwide and is associated with a poor prognosis (21). In addition, HCC frequently becomes aggressively malignant in a short space of time as a result of immunosuppression and the reprogramming of metabolism (22). Accumulating evidence has indicated that a combination of different immunotherapies and targeted therapies can prolong the survival of patients with HCC (23,24). In addition, metabolic reprogramming has been demonstrated to be potentially significant for hepatocarcinogenesis and prognosis (25,26). However, to the best of our knowledge, the mechanism underlying this reprogramming remains unknown (27). One study reviewed the data from immunotherapy trials on HCC (28) and concluded that immunometabolism in the TME exerts an influence on the prognosis of patients with HCC. TP53 mutations result in increased mutational burden in patients with cancer, which may in turn alter the immunometabolism in the TME (29). Therefore, a TP53-associated immune-metabolism signature was developed in the present study for the prediction of HCC prognosis, which may have an increased clinical role in the future.

A recent study has shown that TP53 mutations serve different roles in antitumor immunity (30). In the present study, it was found that the TP53 gene locus had a high mutation frequency in patients with HCC, and the genes modulated downstream of the TP53 mutations were especially enriched for GO terms associated with immune and metabolic responses. Notably, 'tyrosine metabolism' and 'pyruvate metabolism' were markedly downregulated, in addition to the 'alcohol metabolic process' and 'regulation of immune effector process' (Fig. 3C), which may be associated with alcoholic cirrhosis and tumor progression. Since wild-type TP53 serves such fundamental roles in cancer immunity, TP53 mutations can result in immune dysfunction, thereby promoting tumorigenesis, cell invasion and metastasis (31). To deepen the understanding of the changes in immunometabolism in the TME, a nomogram was constructed using the distinctive prognostic signature of ADH4. This nomogram was found to be an effective independent prognostic model for HCC. In addition, it was found that other parameters, including the age of patients and pTNM stage, also significantly affected the OS of patients with HCC. The low-ADH4 group in both mutant and wild-type TP53 groups displayed significantly worse OS time compared with the high-ADH4 group. This suggested that ADH4 is a beneficial signature for the prognosis of HCC where the type of ADH4 is suggested to be wild-type. The ADHs belong to a large family of dehydrogenase enzymes that are associated with good prognoses of various types of cancer, such as colorectal and gastric cancer (32). To investigate the expression profile of ADH4 in HCC, distributions of ADH4 mutants and wild-type ADH4 were compared in the TP53 mutant, wild-type TP53 and total HCC groups. The results revealed that wild-type ADH4 was present in a markedly high proportion of patients with HCC. In conclusion, ADH4 is an immune-metabolic protective factor and low ADH4 can be regarded as a high-risk factor for the prognosis of HCC.

Immune-metabolism relationships have been reported in various diseases, such as cancer, metabolic syndrome and immune-mediated diseases (33). Changes in the TME can also

alter the phenotype and function of immune cells (34). Immune cells have been reported to serve a variety of key roles in the development of malignant tumors, especially in HCC (35). Tumor-infiltrating leukocytes have been reported to impact the progression of HCC (35). In addition, another study found that the functional interaction between tumor-infiltrating T cells and B cells could contribute to local immune activation, improving the prognosis of HCC (35). In the present study, the results indicated that there was significant immune infiltration by B cells and reduced infiltration by T cells in the low risk group, which suggested a differential immune TME. These results suggested that the differential prognosis is associated with the interaction between the TME and the infiltrated immune cells. Furthermore, CD274, CTLA4, HAVCR2, LAG3, PDCD1, PDCD1LG2 and SIGLEC15 were revealed to be immune checkpoint-associated transcripts, which may provide patients with greater benefits from immunotherapy and chemotherapy (36).

The distribution of ADH4 protein expression and the prognostic prediction value were subsequently explored in clinical specimens in the present study. TP53 mutations in serine 249 were revealed, which are associated with high exposure to aflatoxin and poorly differentiated tumors (37). ADH4 protein expression was increased in normal tissues compared with tumor tissues, and patients in the low-ADH4 group had worse OS time compared with those in the high-ADH4 group, which is consistent with the previous analysis (38). This suggested that high-risk patients with HCC are more likely to be involved in ICB responses, which may provide a potentially novel strategy for clinical guidance. However, it should be noted that there were limited numbers of patients for the validation in the present study. In addition, the lack of follow-up data on the 3 patients sampled is also a limitation of the study. The main reason for this limitation is that the 3 patients with HCC were diagnosed in October 2021 and then accepted the surgery. It has been <1 year since successful surgery and the patients are still alive at the time of writing, according to the latest follow-up records. Therefore, larger scale clinical trials would need to be performed to verify the results of the present study. In addition, the mechanism underlying the function of ADH4 and TP53 requires further exploration using gene knockout technology applied in cell line and animal experiments.

To conclude, the present study identified ADH4 to be an immune-metabolism signature downstream of TP53 mutation that can be used to independently predict the prognosis of patients with HCC. Therefore, ADH4 may serve as an accurate biomarker for designing novel immunotherapies.

Acknowledgements

Not applicable.

Funding

This research was supported by a grant from the National Natural Science Foundation of China (grant no. 81874201).

Availability of data and materials

The datasets used and/or analyzed during the current study are available from the corresponding author on reasonable request.

Authors' contributions

YZ made substantial contributions to the conception and the work of manuscript editing. HHJ made substantial contributions to the design of the work. ZYW made substantial contributions to the acquisition and analysis of data. BZ made substantial contributions to conception and approved the modified version. MBL made substantial contributions to the design of the study. BZ and MBL confirm the authenticity of all the raw data. All authors read and approved the final manuscript.

Ethics approval and consent to participate

The research received ethics approval from the Ethics Committee of Renji Hospital (Shanghai, China) and written informed consent was obtained from all participants.

Patient consent for publication

Not applicable.

Competing interests

The authors declare that they have no competing interests.

References

1. Sung H, Ferlay J, Siegel RL, Laversanne M, Soerjomataram I, Jemal A and Bray F: Global cancer statistics 2020: GLOBOCAN estimates of incidence and mortality worldwide for 36 cancers in 185 countries. CA Cancer J Clin 71: 209-249, 2021.
2. Petrick JL, Florio AA, Znaor A, Ruggieri D, Laversanne M, Alvarez CS, Ferlay J, Valery PC, Bray F and McGlynn KA: International trends in hepatocellular carcinoma incidence, 1978-2012. Int J Cancer 147: 317-330, 2020.
3. Pang Y, Liu Z, Han H, Wang B, Li W, Mao C and Liu S: Peptide SMIM30 promotes HCC development by inducing SRC/YES1 membrane anchoring and MAPK pathway activation. J Hepatol 73: 1155-1169, 2020.
4. Bray F, Ferlay J, Soerjomataram I, Siegel RL, Torre LA and Jemal A: Global cancer statistics 2018: GLOBOCAN estimates of incidence and mortality worldwide for 36 cancers in 185 countries. CA Cancer J Clin 68: 394-424, 2018.
5. Jemal A, Ward EM, Johnson CJ, Cronin KA, Ma J, Ryerson B, Mariotto A, Lake AJ, Wilson R, Sherman RL, *et al*: Annual report to the nation on the status of cancer, 1975-2014, featuring survival. J Natl Cancer Inst 109: djx030, 2017.
6. Zheng Y, Chen Z, Han Y, Han L, Zou X, Zhou B, Hu R, Hao J, Bai S, Xiao H, *et al*: Immune suppressive landscape in the human esophageal squamous cell carcinoma microenvironment. Nat Commun 11: 6268, 2020.
7. Wang W and Zou W: Amino acids and their transporters in T cell immunity and cancer therapy. Mol Cell 80 384-395, 2020.
8. Wu J and Cai J: Dilemma and challenge of immunotherapy for pancreatic cancer. Dig Dis Sci 66: 359-368, 2021.
9. Greer RL, Dong X, Moraes AC, Zielke RA, Fernandes GR, Peremyslova E, Vasquez-Perez S, Schoenborn AA, Gomes EP, Pereira AC, *et al*: Akkermansia muciniphila mediates negative effects of IFNγ on glucose metabolism. Nat Commun 7: 13329, 2016.
10. Wu R, Chen F, Wang N, Tang D and Kang R: ACOD1 in immunometabolism and disease. Cell Mol Immunol 17: 822-833, 2020.
11. Mouton AJ, Li X, Hall ME and Hall JE: Obesity, hypertension, and cardiac dysfunction: Novel roles of immunometabolism in macrophage activation and inflammation. Circ Res 126: 789-806, 2020.
12. Donehower LA, Soussi T, Korkut A, Liu Y, Schultz A, Cardenas M, Li X, Babur O, Hsu TK, Lichtarge O, *et al*: Integrated analysis of TP53 gene and pathway alterations in the cancer genome atlas. Cell Rep 28: 1370-1384.e5, 2019.
13. Olivier M, Hollstein M and Hainaut P: TP53 mutations in human cancers: Origins, consequences, and clinical use. Cold Spring Harb Perspect Biol 2: a001008, 2010.

14. Mogi A and Kuwano H: TP53 mutations in nonsmall cell lung cancer. J Biomed Biotechnol 2011: 583929, 2011.
15. Duffy MJ, Synnott NC and Crown J: Mutant p53 as a target for cancer treatment. Eur J Cancer 83: 258-265, 2017.
16. Silwal-Pandit L, Langerød A and Børresen-Dale AL: TP53 mutations in breast and ovarian cancer. Cold Spring Harb Perspect Med 7: a026252, 2017.
17. Yang C, Huang X, Li Y, Chen J, Lv Y and Dai S: Prognosis and personalized treatment prediction in TP53-mutant hepatocellular carcinoma: An in silico strategy towards precision oncology. Brief Bioinform 22: bbaa164, 2021.
18. Meng F, Wu L, Dong L, Mitchell AV, James Block C, Liu J, Zhang H, Lu Q, Song WM, Zhang B, *et al*: EGFL9 promotes breast cancer metastasis by inducing cMET activation and metabolic reprogramming. Nat Commun 10: 5033, 2019.
19. Jiang P, Gu S, Pan D, Fu J, Sahu A, Hu X, Li Z, Traugh N, Bu X, Li B, *et al*: Signatures of T cell dysfunction and exclusion predict cancer immunotherapy response. Nat Med 24: 1550-1558, 2018.
20. Telloni SM: Tumor staging and grading: A primer. Methods Mol Biol 1606: 1-17, 2017.
21. Pinero F, Dirchwolf M and Pessôa MG: Biomarkers in hepatocellular carcinoma: Diagnosis, prognosis and treatment response assessment. Cells 9: 1370, 2020.
22. Golonka RM and Vijay-Kumar M: Atypical immunometabolism and metabolic reprogramming in liver cancer: Deciphering the role of gut microbiome. Adv Cancer Res 149: 171-255, 2021.
23. Sonbol MB, Riaz IB, Naqvi SAA, Almquist DR, Mina S, Almasri J, Shah S, Almader-Douglas D, Uson Junior PLS, Mahipal A, *et al*: Systemic therapy and sequencing options in advanced hepatocellular carcinoma: A systematic review and network meta-analysis. JAMA Oncol 6: e204930, 2020.
24. Llovet JM, Montal R, Sia D and Finn RS: Molecular therapies and precision medicine for hepatocellular carcinoma. Nat Rev Clin Oncol 15: 599-616, 2018.
25. Zhang Y, Yan Q, Gong L, Xu H, Liu B, Fang X, Yu D, Li L, Wei T, Wang Y, *et al*: C-terminal truncated HBx initiates hepatocarcinogenesis by downregulating TXNIP and reprogramming glucose metabolism. Oncogene 40: 1147-1161, 2021.
26. Wang Q, Tan Y, Jiang T, Wang X, Li Q, Dong L, Liu X and Xu G: Metabolic reprogramming and its relationship to survival in hepatocellular carcinoma. Cells 11: 1066, 2022.
27. Jühling F, Hamdane N, Crouchet E, Li S, El Saghire H, Mukherji A, Fujiwara N, Oudot MA, Thumann C, Saviano A, *et al*: Targeting clinical epigenetic reprogramming for chemoprevention of metabolic and viral hepatocellular carcinoma. Gut 70: 157-169, 2021.
28. Machairas N, Tsilimigras DI and Pawlik TM: Current landscape of immune checkpoint inhibitor therapy for hepatocellular carcinoma. Cancers (Basel) 14: 2018, 2022.
29. Mantovani F, Collavin L and Del Sal G: Mutant p53 as a guardian of the cancer cell. Cell Death Differ 26: 199-212, 2019.
30. Li L, Li M and Wang X: Cancer type-dependent correlations between TP53 mutations and antitumor immunity. DNA Repair (Amst) 88: 102785, 2020.
31. Agupitan AD, Neeson P, Williams S, Howitt J, Haupt S and Haupt Y: P53: A guardian of immunity becomes its saboteur through mutation. Int J Mol Sci 21: 3452, 2020.
32. Jelski W and Szmitkowski M: Alcohol dehydrogenase (ADH) and aldehyde dehydrogenase (ALDH) in the cancer diseases. Clin Chim Acta 395: 1-5, 2008.
33. Lercher A, Baazim H and Bergthaler A: Systemic immunometabolism: Challenges and opportunities. Immunity 53: 496-509, 2020.
34. Piñeiro Fernández J, Luddy KA, Harmon C and O'Farrelly C: Hepatic tumor microenvironments and effects on NK cell phenotype and function. Int J Mol Sci 20: 4131, 2019.
35. Garnelo M, Tan A, Her Z, Yeong J, Lim CJ, Chen J, Lim KH, Weber A, Chow P, Chung A, *et al*: Interaction between tumour-infiltrating B cells and T cells controls the progression of hepatocellular carcinoma. Gut 66: 342-351, 2017.
36. Giannone G, Ghisoni E, Genta S, Scotto G, Tuninetti V, Turinetto M and Valabrega G: Immuno-metabolism and microenvironment in cancer: Key players for immunotherapy. Int J Mol Sci 21: 4414, 2020.
37. Nogueira JA, Ono-Nita SK, Nita ME, de Souza MM, do Carmo EP, Mello ES, Scapulatempo C, Paranaguá-Vezozzo DC, Carrilho FJ and Alves VA: 249 TP53 mutation has high prevalence and is correlated with larger and poorly differentiated HCC in Brazilian patients. BMC Cancer 9: 204, 2009.
38. Liu X, Li T, Kong D, You H, Kong F and Tang R: Prognostic implications of alcohol dehydrogenases in hepatocellular carcinoma. BMC Cancer 20: 1204, 2020.
39. Edmondson HA and Steiner PE: Primary carcinoma of the liver: A study of 100 cases among 48,900 necropsies. Cancer 7: 462-503, 1954.